Evaluation of the thermal conductivity and mechanical properties of water blown polyurethane rigid foams reinforced with carbon nanofibers

Santiago-Calvo, Mercedes; Tirado-Mediavilla, Josías; Rauhe, Jens Chr.; Jensen, Lars Rosgaard; Ruiz-Herrero, José Luis; Villafañe, Fernando; Rodríguez-Pérez, Miguel Ángel

Published in:
European Polymer Journal

DOI (link to publication from Publisher):
10.1016/j.eurpolymj.2018.08.051

Publication date:
2018

Document Version
Accepted author manuscript, peer reviewed version

Accepted Manuscript

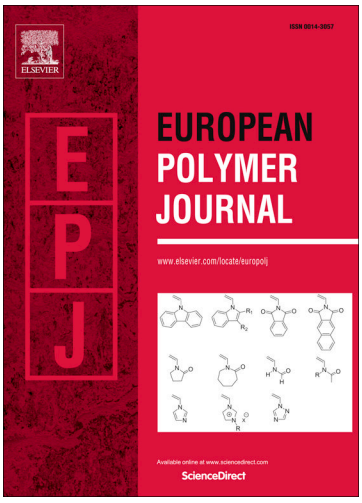

Evaluation of the thermal conductivity and mechanical properties of water blown polyurethane rigid foams reinforced with carbon nanofibers

Mercedes Santiago-Calvo, Josías Tirado-Mediavilla, Jens Chr. Rauhe, Lars Rosgaard Jensen, José Luis Ruiz-Herrero, Fernando Villafañe, Miguel Ángel Rodríguez-Pérez

PII: S0014-3057(18)30898-X
DOI: https://doi.org/10.1016/j.eurpolymj.2018.08.051
Reference: EPJ 8564

To appear in: *European Polymer Journal*

Received Date: 16 May 2018
Revised Date: 18 August 2018
Accepted Date: 27 August 2018

Please cite this article as: Santiago-Calvo, M., Tirado-Mediavilla, J., Rauhe, J.C., Rosgaard Jensen, L., Luis Ruiz-Herrero, J., Villafañe, F., Rodríguez-Pérez, M.A., Evaluation of the thermal conductivity and mechanical properties of water blown polyurethane rigid foams reinforced with carbon nanofibers, *European Polymer Journal* (2018), doi: https://doi.org/10.1016/j.eurpolymj.2018.08.051

Evaluation of the thermal conductivity and mechanical properties of water blown polyurethane rigid foams reinforced with carbon nanofibers

Mercedes Santiago-Calvo[1,*], Josías Tirado-Mediavilla[1], Jens Chr. Rauhe[2], Lars Rosgaard Jensen[2], José Luis Ruiz-Herrero[1], Fernando Villafañe[3], Miguel Ángel Rodríguez-Pérez[1]

1 Cellular Materials Laboratory (CellMat), Condensed Matter Physics Department, Faculty of Science, University of Valladolid, Campus Miguel Delibes 7, 47011 Valladolid, Spain

2 Department of Materials and Production, Aalborg University, Fibigerstraede 16, 9220 Aalborg East, Denmark

3 GIR MIOMeT-IU Cinquima-Química Inorgánica, Faculty of Science, University of Valladolid, Campus Miguel Delibes 7, 47011 Valladolid, Spain

KEYWORD

Polyurethane foam, carbon nanofibers, thermal conductivity, compression test

ABSTRACT

This article studies the effect of carbon nanofibers (CNFs) on the morphological, thermal and mechanical properties of water-blown rigid polyurethane (PUR) foams with densities in the range of 55 to 60 kg/m^3. Different amounts of CNF have been used, 0.1, 0.2, 0.3 and 0.4 wt.%. CNFs are located in the struts and produce minor modifications on open cell content, cell size, cell size distribution and anisotropy ratio of the foams. The contributions of the heat conduction mechanisms have been quantified by measuring the extinction coefficient and by modelling the thermal conductivity. The inclusion of CNFs reduces the radiative contribution by increasing the extinction coefficient and increases the conduction through the solid phase mainly due to an increase in density and an increase of the conductivity of the polymeric matrix. Due to this, a clear reduction of the heat flow by radiation and a reduction of the total thermal conductivity is achieved with only 0.1 wt.% of CNFs. Moreover, the addition of this low amount of CNF allows maintaining the mechanical properties of the foams.

1. Introduction

One of the most important classes of specialty polymers are polyurethanes (PUs) [1]. They are composed by urethanes-linking moieties, obtained by the polyaddition of polyisocyanates to

* Corresponding author.

E-mail address: mercesc@fmc.uva.es (Mercedes Santiago-Calvo).

polyols. PUs may also contain different functional groups in the main chain, such as urea, which come from the reaction of polyisocyanates with the amines resulting from polyisocyanates hydrolysis [2, 3]. PUs are classified according to their chemical structure in thermoplastic polyurethanes (TPU) or thermosets, and according to their physical structure they may be divided into rigid solids, soft elastomers, or foams.

PUs are present in commercial coatings, adhesives, sealants, binders, elastomers and foams [1]. They are considered multipurpose polymers due to the high diversity of PUs, and they cover a surprisingly wide range of applications in areas such as automotive, medical, construction, furniture or appliances, among others [4-7]. Only large-volume commodity plastics such as polyethylene, polypropylene, polyvinyl chloride or polystyrene are ahead of PUs in overall volume used [1]. It is also noteworthy that the demand for PUs is an impressive 7.4% of the whole European polymer market [8].

Most of the PUs industrially obtained are foams, which represent almost 50% of the global foam market [9], mainly due to their interesting physical properties, such as low density, low thermal conductivity, and tailored mechanical properties as a funtion of the foam density. PU foams are usually classified according to their mechanical behaviour into flexible foams (used for furniture, mattresses, and automotive seats) and rigid foams (used for insulation and structural materials) [10].

One of the main applications of rigid polyurethane foams (PUR) is the thermal management for building and transportation insulation or refrigeration systems, where typically the foams are the core of sandwich panels.

The thermal conductivity of foams has been both theoretically [11-19] and experimentally [20-23] studied. The thermal conductivity of a PUR foam (considering both solid and gas phases) is well represented as the addition of conduction in gas and solid phases and radiative conductivity [24].

A method widely used to decrease the thermal conductivity and to improve the mechanical response of PUR foams is the dispersion of fillers into the PU matrix. The characteristics of both foam and additives should be considered in order to select an appropriate reinforcement. Nano-reinforcements can improve the mechanical and thermal properties. Interestingly, this improvement of the composite properties occurs for low contents of nanosize fillers. This is particularly appealing for PUR foams, because the use of a higher amount of filler could preclude the production of foams with the low densities required for thermal insulation and structural applications. The studies published so far in relation to PU nanocomposite foams include the use of different types of nanoparticles, such as nanoclays [20, 25-27], nanosilicas [28, 29], carbon nanotubes [30-34] or carbon nanofibers [35-38]. As expected, these works

lead to conclude that the properties of the final composite depend on both the chemical composition, and on the nanoparticles size, shape, amount added and degree of dispersion and compatibilization obtained.

Carbon nanofibers (CNFs) are cylindrical or conical nanostructures with diameters between 50 and 200 nm and lengths between microns and millimetres. They may present different morphologies, from disordered bamboo-like to highly graphitized ‘‘cup stacked’’ structures [39]. The inclusion of CNFs into polymers produces changes in their thermal and electrical conductivity, tensile and compressive strength, ablation resistance, damping properties, and flammability [40].

Although the addition of CNFs to polymers usually improves the properties of the composites formed, the number of papers dealing with adding CNFs into a rigid PU matrix is somewhat scarce [35-38]. Kabir et al. (2007) studied various process parameters for CNFs sonication dispersion into PUR components, and demonstrated that with the addition of 0.5 and 1 wt.% of CNFs in a PUR system of 240 kg/m^3, the compressive strength was improved by 10% and 20% [38]. Saha et al. (2008) investigated the effects of different nanoparticles (1 wt.% loading with either-TiO_2, platelet nanoclays, or rod-shaped CNFs) introduced by sonication dispersion on the thermal stability and mechanical performances of PUR foam with density 240 kg/m^3. The highest enhancement of both thermal stability and mechanical properties was observed in the system containing 1 wt.% CNFs [35]. Harikrishnan et al. (2010) studied the nanodispersion of CNFs in a PUR system of 35 Kg/m^3, and observed a reduction of thermal conductivity and a clear improvement of compressive modulus and of fire resistance of the nanocomposite foam with 0.5 wt.% of CNFs in the foam, without apparent changes in the foam reaction kinetics [36]. Saha et al. (2011) studied the effect of low amounts of CNF (0.01, 0.05 or 0.1 wt.%) on the reaction kinetics and concluded that the fastest polymerization reaction occurred for the PUR foam containing 0.1% CNF. Moreover, the CNF particles acted as nucleation agents, resulting in a higher number of smaller cells in the composite foam with density 65 Kg/m^3 [37].

The previous papers report that CNFs are promising nanoparticles to improve the properties of PUR foams, however only in one of them the thermal conductivity of the foams is studied. In addition, in that paper [36] the effect of the particles in the heat conduction mechanism is not discussed and the density of the foams analysed is clearly lower than the density of the foams considered in our research.

Keeping the previous ideas in mind, this paper presents a systematic study on the effect of the addition of CNFs on the heat conduction mechanisms of a water-blow PUR system used as the core material of sandwich panels. These foams must have a high compressive strength and due

to this its density is in many cases relatively high (around 55 kg/m^3 in our case). Our target is reducing the thermal conductivity of these foams, which is not an easy task due to the low weight of the radiative contribution (as it is discussed below), while the mechanical properties are at less maintained. Thus, PUR foams containing different amounts of CNFs (0.1, 0.2, 0.3 or 0.4 wt.%) are obtained and their thermal and mechanical properties are measured. Thermal conductivity changes are explained in detail using both theoretical models, measurements of extinction coefficient and a detailed morphological characterization. Moreover, the effect of CNFs on mechanical properties is reported.

2. Experimental

2.1. Materials

The water-blown PUR foams used in this study were obtained from a two-component system supplied by BASF, after mixing the polyol Elastopor H1501/1 and the diphenylmethane diisocyanate ISOPMDI 9240. The polyol is a mixture of components containing polyether polyol, catalysts, stabilizers and water as blowing agent [41, 42].

The vapor grown CNFs were Pyrograf® III PR-24-XT-PS supplied by Applied Sciences Inc. The CNFs has an average diameter of 100 nm and a length of 50-200 microns. Their surface is a minimal chemically vapor deposited (CVD) layer of carbon over a graphitic tubular core [43]. The CNFs were dried in a vacuum oven and stored in a desiccator before use.

2.2. Polyurethane foam and carbon nanofiber-polyurethane foam composite production.

PUR foams containing 0.1, 0.2, 0.3 and 0.4 wt.% of CNFs were obtained as follows. CNFs were firstly added to the polyol by using a Silverson L5M high shear mixer running at 4000 rpm for 30 min. while the mixture was cooled in a water bath to avoid an increase in temperature of the polyol. The isocyanate was added, and the mixture was stirred using a Pendraulik TD100 mechanical mixer running at 2500 rpm for 30s. No difference in reactions between isocyanate and polyol/CNFs mixtures and pure polyol, respectively, was observed indicating that the polyol did not experience a significant heating during the mixing procedure. The mixture was then poured into an open wooden mould with dimensions 250 x 250 x 250 mm^3 and left to foam freely in one direction. The expansion time was 232±21 seconds and the curing temperature was room temperature. After 24 hours the foam was demoulded and cut into appropriate dimensions using a bandsaw. The cured samples were also stored at room temperature before testing. PUR foams without CNFs were also obtained as a reference. In all cases the polyol and isocyanate were mixed in a ratio 100:160 by weight, so each foam

formulation was fixed with the same total amount of components (isocyanate, polyol, catalyst, water and other additives).

2.3. Carbon nanofibers characterization

1 wt. % of CNFs were dispersed in tetrahydrofuran using a sonicator horn for 30s. Small drops of the solution were placed on the SEM specimen holders and the tetrahydrofuran was removed by drying in a fume hood overnight leaving CNFs dispersed on the holders. The diameters of the fibers were determined using a Zeiss EVO LS15 scanning electron microscope and ImageJ.

2.4. Foam characterization

2.4.1. Density

Foam density was measured as described by ASTM D1622/D1622M-14 [44]. Density was determined by dividing the weight of each sample by its corresponding volume of five different samples for each material. The samples were cylindrical with a diameter of 30 mm and a height of 25 mm.

2.4.2. Open cell content

The percentage of open cell content (OC) was measured with a gas pycnometer Accupyc II 1340 from Micromeritics, according to ASTM D6226-10 [45]. Nitrogen is used as the displacement medium. The OC was measured for five cylindrical samples from each material after measuring their densities. OC was calculated by using the following equation [45]:

$$OC\ (\%) = 100\left(\frac{V_{Sample} - V_{Pycnometer}}{V_{Sample}\ p}\right) \qquad (1)$$

Where V_{sample} is the geometrical volume of the sample (calculated from the sample dimensions), $V_{pycnometer}$ is the volume measured with the pycnometer, p is the sample porosity calculated using $\left(1 - \frac{p_{foam}}{p_{solid}}\right)$, where p_{foam} is the foam density and p_{solid} the solid matrix density. A value of 1160 kg/m^3 was used as p_{solid}.

2.4.3. Morphological characterization of foams

Optical Microscopy (OM) was used to locate the position of CNFs in the foam structure. Optical micrographs were taken using a Leica DM2500M microscope.

Scanning electron microscopy (SEM) was used to characterize the cellular structure of the foam (cells, cell walls, and struts). SEM micrographs were taken with a JEOL JSM-820 microscope. The foams were cut with blades to ensure a smooth surface, which was examined by SEM after vacuum coating with a gold monolayer. SEM micrographs were obtained in the growth plane of the foam.

The main characteristics of the cellular foam structure were determined by an image analysis technique [46] . The Image analysis was carried out with ImageJ by measuring at least 400 cells. Cell size distribution, average cell size (Φ_{3D}) and anisotropy ratio (AR) were thus determined. In addition, some statistical parameters of the cell size distribution were calculated: standard deviation (SD), normalized standard deviation (NSD), and the asymmetry coefficient (AC). NSD (ratio between SD and Φ_{3D}) is related to the width of the cell size distribution, and therefore provides information about the homogeneity of the cell size distribution (i.e. homogeneous cell distributions present small values of NSD). AC provides information about the shape of distribution, a negative coefficient indicating that the smallest cells are more separated from the average cell size value than the biggest ones, and *vice versa.*

2.4.4. Fourier transform infrared (FTIR) spectroscopy

FTIR spectra of the samples were collected using a Bruker Tensor 27 spectrometer by transmission method. Chemical reactivity between nanoparticles and PUR foam was analyzed using FTIR.

2.4.5. Thermal conductivity

The thermal conductivity measurements of the foams were performed using a Rapid K heat flowmeter from Holometrix. Measurements were made under steady heat flow conditions through the test samples, in accordance with the UNE12667 method [47], by using samples of 200 x 200 x 25 mm, after calibrating with a standard sample. Thermal conductivity (λ) was calculated by measuring the heat flow through the test sample, q, as a result of the temperature gradient (ΔT) across the growth plane of material. λ was calculated according to Fourier's equation [47]:

$$q = \lambda A \frac{\Delta T}{\mathrm{d}} \qquad (2)$$

Where *d* is sample thickness, and *A* is the cross-sectional area of the sample calculated from a standard sample. The measurements were performed at 20°C, with a temperature gradient (ΔT) of 10°C. Thermal conductivity for each sample was measured 7 times, each one during 10

minutes, in order to obtain an average value. These measurements were performed six months after the foams were produced, considering that by then all the carbon dioxide generated during foaming should have been diffused out to the atmosphere, and therefore the only gas inside the foams is air.

2.4.6. Mechanical Tests

Mechanical tests were performed according to ASTM D1621-10 [48]. These experiments were performed in compression using an Instron Machine (model 5.500R6025). Stress-strain curves were obtained at room temperature at a strain rate of 10 mm/min. The maximum static strain was 75% for all the experiments and the compression direction was parallel to the cell growth direction (thickness direction) of the foam. The samples were cylindrical with a diameter of 30 mm and a height of 25 mm. Young´s modulus (E) and collapse stress (σ_C) were measured.

2.4.7. Spectral extinction coefficient ($K_{e,\lambda}$)

Sample thickness *(L)* and transmission measurements *(τ)* are needed to determine the spectral extinction coefficient ($K_{e,\lambda}$).

Sample Thickness (L)

Five to seven thin samples with a thickness (L) ranging between 0.8 and 2.5 mm were cut from the five different foams studied. A dynamic mechanical analyzer (DMA7) from PerkinElmer was used to measure the thickness (L) of the samples with a high accuracy. A parallel-plate system with a top plate of 12 mm in diameter was used applying a force of 10 mN.

Transmission measurements (τ)

Spectra of the thin samples were collected using a Bruker Tensor 27 FTIR spectrometer in the transmission mode. The spectra were obtained after 32 scans with a resolution of 4 cm^{-1} in a wavenumbers range from 4000 and 400 cm^{-1}, after subtracting a background spectrum. The data supplied by the software were a collection of 1866 values in this range. The samples were located as close as possible to the detector in our device in order to minimize the loss of transmitted intensity due to the scattering of radiation. This is the same approach used in our previous research in which the same type of characterization was performed [24, 49].

The transmittance (τ) is the ratio of the intensity transmitted through the sample ($I_\lambda(x)$) with respect to the intensity without the sample ($I_{0,\lambda}$):

$$\tau_{n,\lambda} = \frac{I_\lambda(x)}{I_{0,\lambda}} \quad (3)$$

The spectral extinction coefficient ($K_{e,\lambda}$) for thin samples can be obtained from Beer's law [50]. For homogeneous samples, once $K_{e,\lambda}$ is assumed to be independent of sample thickness, the following equation is valid:

$$\tau_{n,\lambda} = e^{(-\int_0^L K_{e,\lambda} dx)} \quad (4)$$

Therefore, the spectral extinction coefficient ($K_{e,\lambda}$) can be expressed from the spectral transmittance $\tau_{e,\lambda}$ as:

$$K_{e,\lambda} = \frac{-\ln(\tau_{n,\lambda})}{L} \quad (5)$$

As a result, $K_{e,\lambda}$ can be obtained by means of a linear regression of the plot of $ln(\tau_{e,\lambda})$ *vs*. *L*.

3. Results and discussion

3.1. Foams characterization

The cellular structure and some physical properties of the foams are collected in Table 1. The density slightly increases up to around 5 kg/m^3 when low amounts of CNFs are added (Table 1). Since each system contains the same total amount of components, the small increase in density is connected with the progressive increase in the viscosity of the CNF/polyol mixture when the particles are added which reduces the volume expansion of the foams. In addition to density, the open cell content (OC) slightly increases from 8.9% up to 10.8% with CNFs addition (Table 1) which indicates that the particles are not acting as cell openers due to both their poor compatibility with the PU matrix and their lack of chemical reactions with PU formulation components, as discussed below.

Figure 1 shows SEM images of the microcellular structure of samples, whereas the average cell size (Φ_{3D}) as a function of CNF amount is presented in Figure S1. It is observed that the changes in cell size are very small when CNFs are incorporated in PU formulation. The cell size is reduced a 6% for the foam containing 0.2 wt.% CNFs, whereas increases a 7% for those samples with higher amounts of CNFs (0.3 and 0.4 wt.% CNFs) may be due to bubble coalescence, which is evidenced qualitatively in the SEM micrographs.

Moreover, there are hardly changes in the cell size distribution. Gaussian fitting of the distributions is displayed in Figure S2. All samples show relatively high homogeneity (small values of NSD) and positive AC (large cell are more separated from mean cell size than smallest

cells) (Table 1). Additionally, anisotropy ratio (AR) values are also included in Table 1. All the foams have a certain degree of anisotropy in the thickness direction, but no trends as a function of the CNF content are observed.

Based on the results obtained, it is concluded that, the effect of CNFs in the cellular structure of the foams is small.

Table 1. Main cellular structure characteristics and physical properties of the manufactured PU foams: density, open cell content (OC), mean cell size (Φ_{3D}), standard deviation of the cell size distribution (SD), normalized standard deviation (NSD), asymmetry coefficient (AC) and anisotropy ratio (AR).

Samples	Density (Kg/m^3)	OC (%)	Φ_{3D} (µm)	SD	NSD	AC	AR
Pure	56.2±0.9	8.9±0.7	366	169	0.46	0.80	1.22±0.34
0.1%CNF	59.9±0.5	8.7±0.6	359	141	0.48	0.79	1.21±0.39
0.2%CNF	58.4±1.3	10.4±0.4	346	146	0.42	0.63	1.38±0.39
0.3%CNF	60.7±0.8	10.5±0.1	392	191	0.49	2.12	1.21±0.32
0.4%CNF	60.8±0.5	10.8±0.4	390	174	0.45	0.83	1.26±0.37

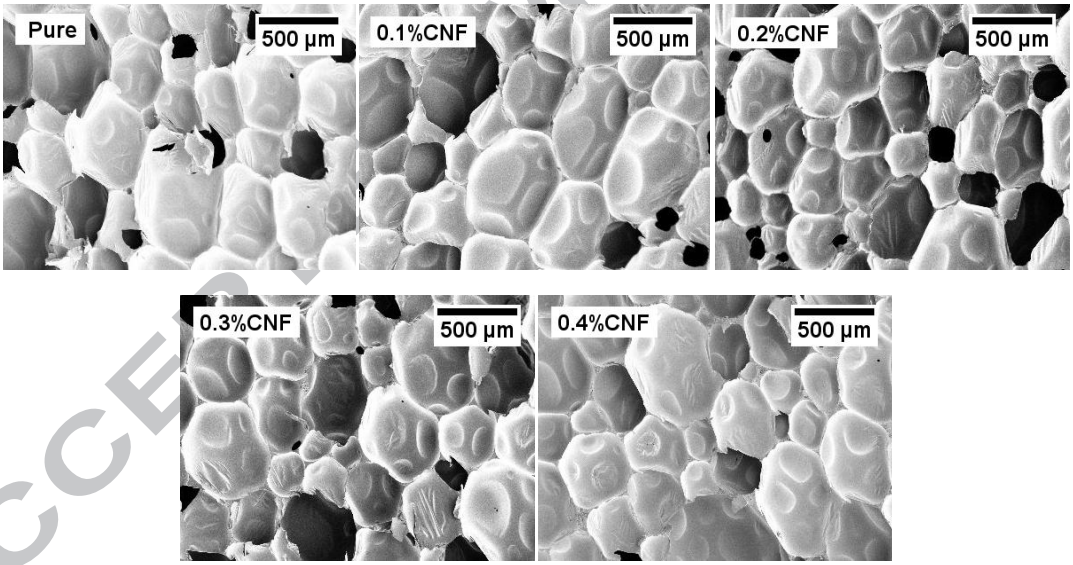

Figure 1. SEM micrographs in the growth plane of the foams: Pure material, with 0.1 wt.% CNFs, with 0.2 wt.% CNFs, with 0.3 wt.% CNF and with 0.4 wt.% CNFs.

3.2. CNFs characterization and distribution in the foam

A representative SEM image of the CNFs and a diameter distribution plot are shown in Figure 2. The characterization of the dimensions of CNFs gave an average diameter of 102 nm, with a standard deviation of 26 nm. Besides CNFs the material used as filler also contains small

amounts of other particles such as iron catalyst particles as it can be appreciated in Figure 2 [43].

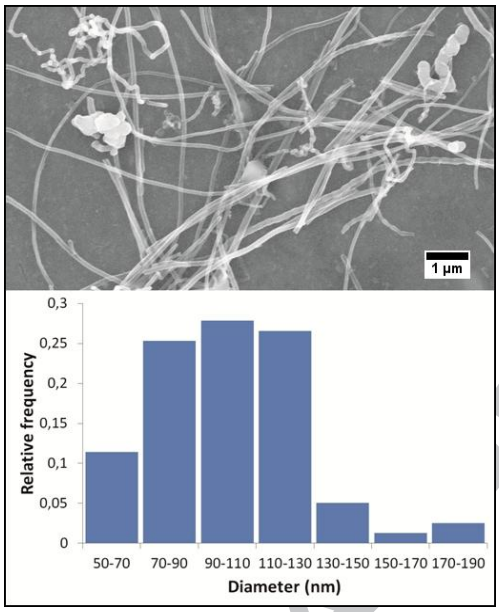

Figure 2. SEM micrograph and diameter distribution of carbon nanofibers.

CNFs could act as infrared radiation absorbent [51], and therefore their localization in the foam is important in order to understand its influence on the thermal conductivity. The solid phase in cellular materials is distributed between the two components of cells: walls and struts, and consequently the CNFs could be located in both areas. Figure 3 shows optical micrographs for the foam containing 0.4 wt.% CNF (the results obtained for the other foams containing CNFs were similar). The cell walls are free from nanoparticles, whereas the CNFs can be only observed in the struts (Figure 3.b). On the other hand, the SEM micrographs in Figure 4 confirm that the nanoparticles are mainly situated in the struts, whereas only small amounts of particles are present in the cell walls (Figure 4.a and 4.b). These results were common for all the materials containing CNFs. Moreover, the poor adhesion of the CNFs in the PU matrix is also observed in the SEM images shown in Figure 4.c and 4.d. This poor adhesion between the filler and the matrix could play a role on the mechanical response of the foams, as discussed below.

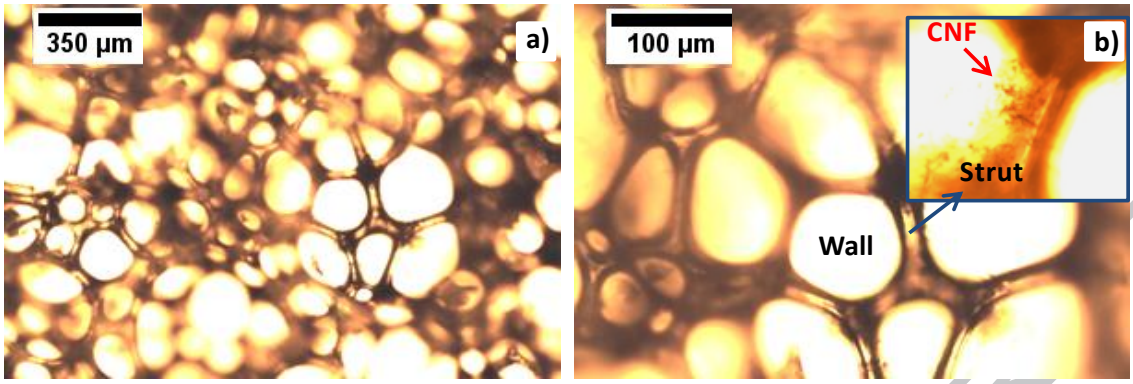

Figure 3. Optical microscopy images of the microstructure for PUR foam with 0.4 wt.% CNF. (a) General view, (b) Enlarged image showing cell walls and struts.

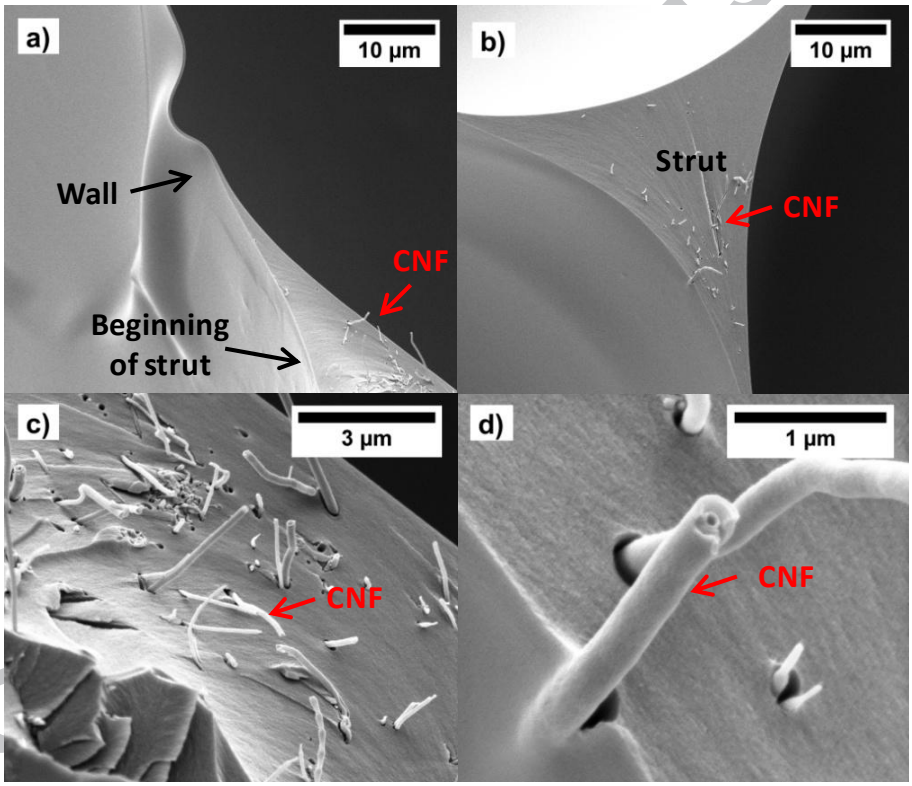

Figure 4. SEM micrographs of the microstructure for PUR foam with 0.3%CNF. (a) Wall and beginning of a strut, (b) Strut, (c) CNFs in the strut, (d) CNFs in the strut (detail).

In conclusion, both optical and SEM micrographs show that CNF nanoparticles are mainly located in the struts. A possible explanation of this result is that the cell wall thickness in these foams is in the range of 1 to 2.5 microns and the size of the struts is slightly higher, as a result the CNFs cannot be located in the walls because although they have an average diameter of 102 nm, their length is high, between 50 and 200 microns. In addition, the CNFs have a minimal chemically vapor deposited (CVD) layer of carbon on the surface, and therefore their

surface hardly have functional groups which can react with other functional groups present in foam components, such as isocyanate, polyols or the blowing agent (water) [36]. This lack of chemical reaction between CNFs and foam components does not allow to redistribute the CNFs along cell walls and may also explain the poor adhesion of the CNFs present in the foam. Besides, the pure PUR foam and the PUR foams containing CNFs display the same absorptions in the FTIR spectra (Figure 5), supporting the no chemical reaction between the CNFs and the PU matrix.

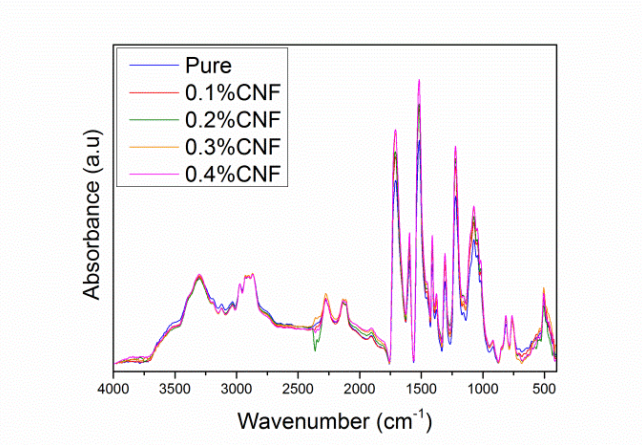

Figure 5. FTIR spectra of the PUR foams.

3.3. Study of thermal conductivity

The thermal conductivity was measured once carbon dioxide has diffused outside the cells and has been substituted by atmospheric air [24]. Table1 and Figure 6 show the thermal conductivity values obtained once this final stationary state has been reached. The thermal conductivity for the reference foam is 35.6 mW/mK. This value is in the range expected considering that the foam is water-blown, so air was in the cells when the conductivity was measured, and taking into account that the density is relatively high, 56 kg/m^3. Reducing the thermal conductivity of this foam, while keeping a high density, is not a simple task because as it will be explained later the radiative contribution (the one that it is possible to reduce by using the CNFs) has a low contribution in these systems. Despite this fact, a small number of particles (0.1 wt.%) can reduce the thermal conductivity to values of 34.8 mW/mK (Figure 6). Therefore, a small content of particles is needed to detect a clear reduction of the thermal conductivity. However, only this small amount can improve the results, increasing this content to values of 0.2, 0.3 or 0.4 wt.% does not further reduce the thermal conductivity.

As it is shown in Table 1, the inclusion of CNFs causes insignificant changes in the density, open cell content, cell size, anisotropy and cell size distribution, so that the variations in thermal

conductivity cannot be explained by variations of these parameters. Thus, in order to understand the results obtained a detailed study considering measurements of the extinction coefficient and modelling of the thermal conductivity modelling has been carried out.

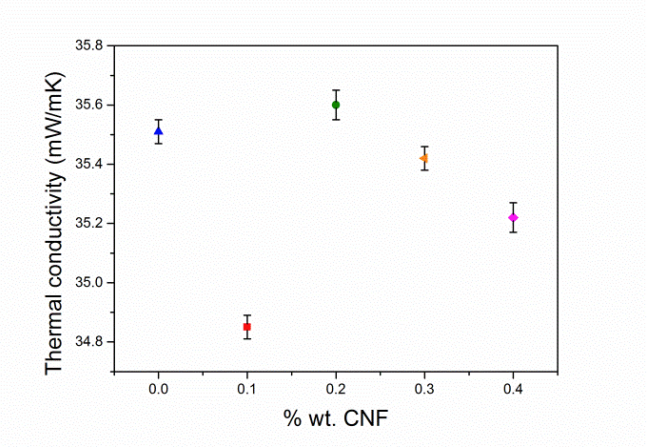

Figure 6. Thermal conductivity as a function of CNF concentration.

3.3.1. Rosseland extinction coefficient (K_R)

When thick PUR foams are used in real applications, the mean free path for radiation propagation is small enough to be considered as an optically thick medium. Radiative heat transfer through an optically thick medium can be estimated by the diffusion approximation where the radiative heat flux $q_r(x)$ is proportional to the black body emissive power (σT^4), and can be expressed as follows [11]:

$$q_r(x) = \frac{4}{3K_{e,R}}\frac{\partial e_b}{\partial x} = \frac{-16\sigma T^3}{3K_{e,R}}\frac{\partial T}{\partial x} = -\lambda_r \frac{\partial T}{\partial x} \qquad (6)$$

λr is the radiative conductivity, σ is the Stefan–Boltzmann constant, T is the mean temperature, and $K_{e,R}$ is the Rosseland mean extinction coefficient. Hence, the radiative conductivity can be approximated by the Rosseland equation [11]:

$$\lambda_r = \frac{16n^2\sigma T^3}{3K_{e,R}} \qquad (7)$$

Where *n* is the effective refraction index, and $K_{e,R}$ is the Rosseland mean extinction coefficient. In this case, *n* is close to one because the volume of gas (porosity) of the PUR foams herein studied is approximately 95%. $K_{e,R}$ is obtained from the following equation [50]:

$$\frac{1}{K_{e,R}} = \frac{\int_0^\infty \frac{1}{K_{e,\lambda}} \frac{\partial e_{b,\lambda}}{\partial T} d\lambda}{\int_0^\infty \frac{\partial e_{b,\lambda}}{\partial T} d\lambda} \quad (8)$$

Where $e_{b,\lambda}$ is the spectral blackbody emissive power and λ is the wavelength. Therefore, the Rosseland mean extinction coefficient is an average value of $K_{e,\lambda}$ weighed by the local spectral energy flux. Once, $K_{e,\lambda}$ is measured experimentally (equations 4 and 5), $K_{e,R}$ can be obtained using equation 8.

The Rosseland mean extinction coefficients obtained for each sample are shown in Figure 7 and clearly increase when increasing the amounts of CNFs. There is clear increase up to 0.3 wt.% of CNF content and then the values are stable. The trend of Rosseland extinction coefficient should be due to an increase of the extinction coefficient of the PU matrix due to the presence of CNFs because the cellular structure is similar for all the analyzed foams. All this will imply a reduction of the radiative contribution of thermal conductivity for samples with CNFs, as discussed later.

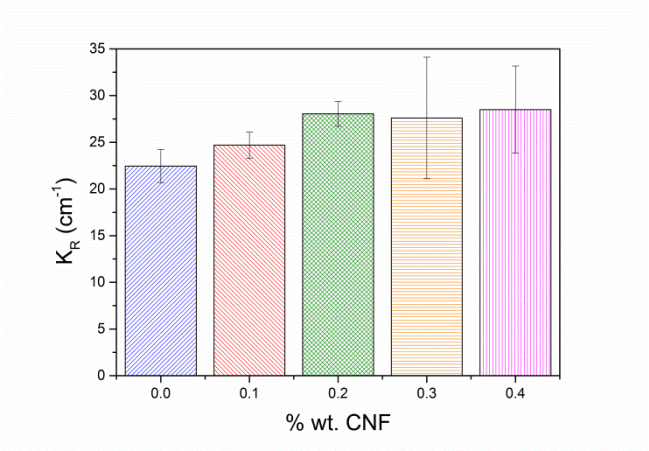

Figure 7. Experimental results for Rosseland extinction coefficient (K_R).

3.3.2. Thermal conductivity modelling

The thermal conductivity of the PUR foam (containing solid and gas phases) is well represented by the addition of four heat conduction mechanisms: conduction along the cell walls and the struts of the solid polymer (λ^s), conduction through the gas phase (λ^g), thermal radiation (λ^r), and convection within the cells (λ^c). The addition of these contributions gives the total thermal conductivity (λ^t):

$$\lambda^t = \lambda^s + \lambda^g + \lambda^r + \lambda^c \quad (11)$$

The convective mechanism is considered negligible [11] due to the very small cell size of the foams under study (300-400 μm). The conductive terms of the gas and of the solid phases can be estimated by equations 12 and 13:

$$\lambda^g = \lambda_g V_g \quad (12)$$

$$\lambda^s = \lambda_s \frac{V_s}{3}\left(\left(f_s\sqrt{AR}\right) + 2(1-f_s)(AR)^{1/4}\right) \quad (13)$$

where V_g is the volume fraction of the gas phase ($1-\rho_f/\rho_s$), ρ_f and ρ_s are the density of the foams and the density of the solid respectively (ρ_s =1160 kg/m^3), V_s is the volume fraction of the solid phase (ρ_f/ρ_s), *AR* is the anisotropy ratio, λ_g is the thermal conductivity of the gas for a given temperature, and λ_s is the thermal conductivity of the solid matrix that is unknown for the materials under study because the effect of the nanoparticles on this property cannot be measured [17]. The gas conduction (equation 12) depends on the nature of the gas. As indicated above, the gas inside the cells once the final stationary state has been reached is atmospheric air, whose conductivity at 20°C is 25.6 mW/mK [52].

3.3.3. Estimation of heat conduction mechanisms.

An estimation of the different heat conduction mechanisms for the samples under study was conducted. The conductivity through the gas phase was calculated using equation 12 and the radiative contribution was obtained using equation 7 and the experimental values measured for the extinction coefficient. The conduction through the solid phase was calculated as difference between the experimental thermal conductivity and the values of conduction in the gas phase and radiation. We used this procedure because the thermal conductivity of the solid matrix λ_s is unknown.

Figure 8 shows the contribution (in percentage) of each heat conduction mechanism.

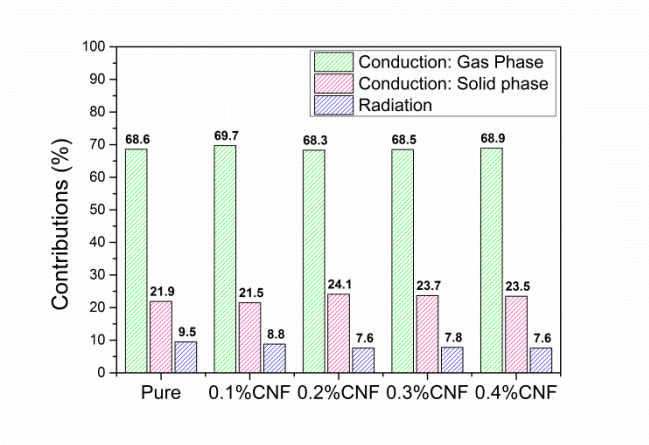

Figure 8. The contribution of the thermal conductivity mechanisms for each PU foam.

3.3.3.1. Modelling discussion: Conduction through the gas phase

As shown by Figure 8 this contribution is the most significant in the final value of the thermal conductivity. As explained above, the thermal conductivity is measured when the composition of the gas in the cells has reached a stationary value, i.e. when all carbon dioxide (conductivity = 14.5 $mWm^{-1}K^{-1}$) has diffused outside the cells and has been replaced by atmospheric air (25.6 $mWm^{-1}K^{-1}$). Using the thermal conductivity model (equation 11), the conduction through the gas phase with 100% of air concentration inside the cells is app.69% for the all the materials under study(Figure 8).

3.3.3.2. Modelling discussion: Radiation term

The radiative conductivity can be estimated by the Rosseland equation (equation 11) using the Rosseland extinction coefficient ($K_{e,R}$) obtained experimentally. The radiative contribution is app. 10% for the pure material, and the addition of CNFs results in a decrease of this contribution from 10% to around 8% (Figure 8). Since the radiative conductivity is associated with changes in the extinction coefficient (cellular structure did not change when CNFs were added), the increase of extinction coefficient with CNFs addition previously discussed involves a high reduction of radiative conductivity up to 20% for the material containing CNFs. Therefore, it is concluded that a very small content of CNFs is enough to have a second phase that is acting in a very effective way as infrared blocker. It is important to remark here that the relatively high density of the foam system under study (56 kg/m^3) results in a low contribution of the radiative heat transfer, only 10%, much lower than the 20% reached for foams systems with lower densities [53-55]. Due to this reason and, as it was mentioned in the introduction, it is not an easy task to reduce the conductivity of this type of PU systems by using strategies

acting on the radiative heat conduction. In this system the maximum reduction of the total thermal conductivity we could reach is 10% by completely removing the heat conduction by radiation. Therefore, the result obtained, a reduction of 20% of the radiative contribution that translates into a 2.2% reduction of the total conductivity for the material containing 0.1 wt.% of CNFs is considered a promising result.

3.3.3.3. Modelling discussion: Conduction through the solid phase

The contribution of conduction through the solid gives app. 22% for the pure PUR foam and increases as CNFs concentration grows (Figure 8). The relatively high density of the foams under study is the reason behind this high contribution of the solid phase [53-55]. On the one hand, the density of the foam increases when the fillers are added (see Table 1) and this is one of the reasons justifying the increase of this contribution when filler content increases. On the other hand, Table 2 collects the thermal conductivity of the polymeric matrix (λs) for all samples, which is calculated by using the thermal conductivity model (equation 11) and the values of the heat conduction through the solid phase (Figure 8). As it can be seen, λs in the materials containing nanofillers increases with the CNFs contents (0.2 and 0.3 wt.%). This is probably due to an increase of the conductivity of the solid matrix due to the formation of an interconnected network of the fibers [32, 33].

Table 2. Thermal cconductivity of the polymeric matrix (λs) for the samples containing nanoparticles.

Samples	λs (mW/mK)
Pure	342
0.1%CNF	311
0.2%CNF	347
0.3%CNF	345
0.4%CNF	334

In summary, this analysis indicates that the addition of CNF particles causes an increase of the extinction coefficient, due to the activity of the particles as infrared blockers, and at the same time an increase of the conduction through the solid phase due to the increase in density of the foam and increase of the conductivity of the polymeric matrix. The optimum material is the one containing 0.1 wt.% CNF because in this system the particles are acting as IR blockers and the solid phase contribution is still low. For higher contents of particles, the increase in the solid phase contribution compensates the increase of the extinction coefficient, resulting in materials with a similar conductivity to that of the pure foam.

3.4. Mechanical properties

The compressive properties (Young's modulus and collapse stress) of PUR foams were measured at room temperature. The Gibson and Ashby relationship between mechanical properties and density [56] must be used in order to exclude the differences in densities between the foam samples. Therefore, Young's modulus and collapse stress divided by the relative density of the foam samples allow the comparison of the mechanical properties of the PU foams with different CNFs content. The relative Young's modulus and relative collapse stress of the foams are collected in Figures 9. It can be observed that the mechanical properties are hardly modified by the CNFs because the cellular structure of nanocomposite foams is not deteriorated by the addition of the particles. The slightly reduction of relative collapse stress for foams with CNFs could be due to the poor adhesion of CNFs to the PU matrix. The most interesting result is for the foam containing 0.1 wt.% CNFs which slightly increases (8%) the relative Young's modulus and maintains the relative collapse stress, in addition to the reduction of the thermal conductivity reported in previous paragraphs. This result is remarkable because in several studies [25, 57-59] the inclusion of nanoparticles into PU foams improves some properties such as the thermal conductivity, however the mechanical properties are reduced [58, 59].

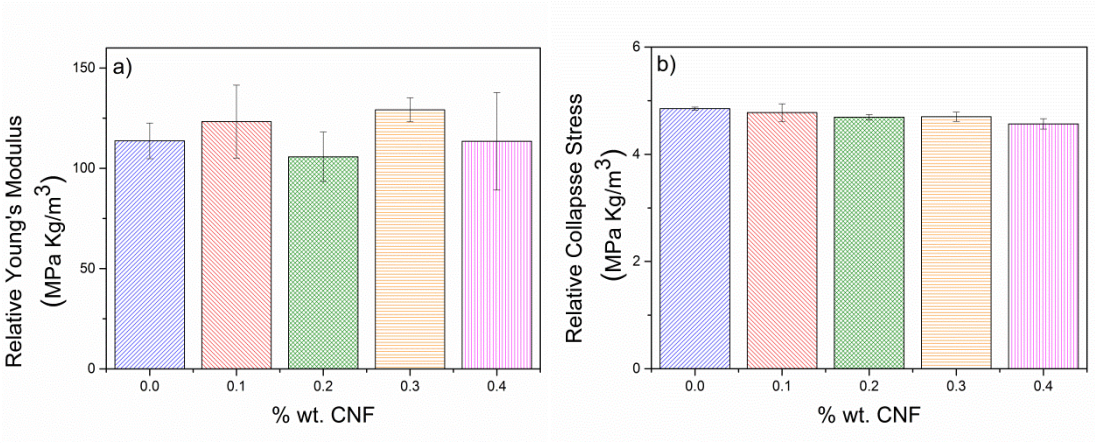

Figure 9. a) Relative Young's modulus and b) relative collapse stress for the foams corresponding to compression tests.

4. Conclusions

PUR foams with densities in the range of 55-60 kg/m^3 reinforced with small amounts of CNFs have been prepared and characterized. The cellular structure of the foams slightly changes due to the addition of CNFs. These nanoparticles are mainly situated in the struts and have a poor adhesion with the PU matrix.

The inclusion of CNFs increases the extinction coefficient of the foam, and as consequence there is a clear reduction of radiative contribution of the thermal conductivity for the samples containing CNFs (up to 20%). The total thermal conductivity is reduced at very low contents of CNFs (0.1 wt.% of CNFs content). For this material thermal conductivity is reduced by 2% in comparsion with the reference foam, which is a remarkable result taking into account that the foams under stuyd have relatively high densities. Concentrations higher than 0.1 wt.% do not lead to higher reductions of the thermal conductivity due to an increase of the heat conduction through the solid phase, which is due to a density increase when the particles are added and to an increase of the thermal conductivity of the solid matrix. On the other hand, the sample with 0.1 wt.% of CNFs, in addition to the improved thermal insulation, presents a slight increase in relative Young's modulus and maintains the relative collapse stress.

Acknowledgement

Financial assistance from MINECO, FEDER, UE (MAT2015-69234-R) and the Junta de Castile and Leon (VA011U16) are gratefully acknowledged.

Data Availability

The raw/processed data required to reproduce these findings cannot be shared at this time as the data also forms part of an ongoing study.

References

[1] M. Szycher, Szycher's Handbook of Polyurethanes, Second ed., CRC Press 2012.
[2] K. Ashida, Polyurethane and related foams: Chemistry and Technology, CRC Press 2007.
[3] H.W. Engels, H.G. Pirkl, R. Albers, R.W. Albach, J. Krause, A. Hoffmann, H. Casselmann, J. Dormish, Polyurethanes: versatile materials and sustainable problem solvers for today's challenges, Angew. Chem., 52 (2013) 9422-9441.
[4] U. Meier-Westhues, Polyurethanes: Coatings, Adhesives and Sealants., Vincentz Network, Hannover, 2007.
[5] N.M.K. Lamba, K.A. Woodhouse, S.L. Cooper, Polyurethanes in Biomedical Applications, CRC Press, Boca Raton, Fl, US, 1997.
[6] R.M. Evans, Polyurethane sealants: technology and applications, Technomic Publishing Company, Lancaster, PA, 1993.
[7] S. Lee, Thermoplastic Polyurethane Markets in the EU: Production, Technology, Applications and Trends, Rapra Technology Limited, United Kingdom, 1998.
[8] Plastics-the Facts 2014. An analysis of European plastics production, demand and waste data for 2014., in: PlasticsEurope (Ed.), 2015.
[9] Polymer Foams Market Expected to Consume 25.3 Million Tonnes by 2019. http://www.smithersrapra.com/news/2014/may/polymer-foam-market-to-consume-25-3-million-tonnes, 2014 (accessed 18 August 2018).
[10] D. Klempner, V. Sendijarevic, Handbook of Polymeric Foams and Foam Technology, Hanser 1991.

[11] L. Glicksman, Low Density Cellular Plastics: Physical Basis of Behaviour, Springer Netherlands, London, 1994.
[12] R.J.J. Williams, C. Aldao, Thermal Conductivity of Plastic Foams, Polym. Eng. Sci., 23 (1983) 293–298.
[13] R. Boetes, C.J. Hoogendoorn, Heat Transfer in Polyurethane Foams for Cold Insulation, Proceedings of the International Centre for Heat and Mass Transfer, 1987, pp. 14-20.
[14] J. Francl, W.D. Kingery, Thermal Conductivity: IX, Experimental Investigation of Effect of Porosity on Thermal Conductivity, J. Am. Ceram. Soc., 37 (1954) 99–107.
[15] M.A. Schuetz, L.R. Glicksman, A Basic Study of Heat Transfer Through Foam Insulation, J. Cell. Plast., 20 (1984) 114-121.
[16] L. Glicksman, M. Schuetz, M. Sinofsky, Radiation heat transfer in foam insulation, Int. J. Heat Mass Transfer., 30 (1987) 187–197.
[17] L.R. Glicksman, Heat transfer and ageing of cellular foam insulation, J. Cell. Plast., 10 (1991) 276-293.
[18] O.A. Almanza, M.A. Rodríguez-Pérez, J.A.D. Saja, Prediction of the radiation term in the thermal conductivity of crosslinked closed cell polyolefin foams, J. Polym. Sci. Part B: Polym Phys, 38 (2000) 993–1004.
[19] J. Kuhn, H.P. Ebert, M.C. Arduini-Schuster, D. Büttner, J. Fricke, Thermal transport in polystyrene and polyurethane foam insulations, Int. J. Heat Mass Transfer., 35 (1992) 1795-1801.
[20] S.H. Kim, M.C. Lee, H.D. Kim, H.C. Park, H.M. Jeong, K.S. Yoon, B.K. Kim, Nanoclay reinforced rigid polyurethane foams, J. Appl. Polym. Sci., 117 (2010) 1992-1997.
[21] J.W. Wu, W.F. Sung, H.S. Chu, Thermal conductivity of polyurethane foams, Int. J. Heat Mass Transfer., 31 (1999) 1100–1106.
[22] M.S. Han, S.J. Choi, J.M. Kim, Y.H. Kim, W.N. Kim, H.S. Lee, J.Y. Sung, Effects of Silicone Surfactant on the Cell Size and Thermal Conductivity of Rigid, Macromol. Res., 17 (2009) 44–50.
[23] C.-j. Tseng, M. Vamaguch, T. Ohmori, Thermal conductivity of polyurethane foams from room temperature to 20 K, Cryogenics, 37 (1997) 305–312.
[24] S. Estravís, J. Tirado-Mediavilla, M. Santiago-Calvo, J.L. Ruiz-Herrero, F. Villafañe, M.A. Rodríguez-Pérez, Rigid polyurethane foams with infused nanoclays: Relationship between cellular structure and thermal conductivity, Eur. Polym. J., 80 (2016) 1–15.
[25] X. Cao, L. James Lee, T. Widya, C. Macosko, Polyurethane/clay nanocomposites foams: processing, structure and properties, Polymer, 46 (2005) 775–783.
[26] Z. Xu, X. Tang, A. Gu, Z. Fang, Novel preparation and mechanical properties of rigid polyurethane foam/organoclay nanocomposites, J. Appl. Polym. Sci., 106 (2007) 439-447.
[27] G. Harikrishnan, T.U. Patro, D.V. Khakhar, Polyurethane Foam-Clay Nanocomposites: Nanoclays as Cell Openers, Ind. Eng. Chem. Res., 45 (2006) 7126–7134.
[28] M.M.A. Nikje, Z.M. Tehrani, Polyurethane Rigid Foams Reinforced by Doubly Modified Nanosilica, J. Cell. Plast., 46 (2010) 159–172.
[29] M.M.A. Nikje, Z.M. Tehrani, Thermal and mechanical properties of polyurethane rigid foam/modified nanosilica composite, Polym. Eng. Sci., 50 (2010) 468–473.
[30] L. Zhang, E.D. Yilmaz, J. Schjødt-Thomsen, J.C. Rauhe, R. Pyrz, MWNT reinforced polyurethane foam: Processing, characterization and modelling of mechanical properties, Compos. Sci. Technol., 71 (2011) 877-884.
[31] D. Yan, L. Xu, C. Chen, J. Tang, X. Ji, Z. Li, Enhanced mechanical and thermal properties of rigid polyurethane foam composites containing graphene nanosheets and carbon nanotubes, Polym. Int., 61 (2012) 1107-1114.
[32] D.-X. Yan, K. Dai, Z.-D. Xiang, Z.-M. Li, X. Ji, W.-Q. Zhang, Electrical conductivity and major mechanical and thermal properties of carbon nanotube-filled polyurethane foams, J. Appl. Polym. Sci., 120 (2011) 3014-3019.

[33] N. Athanasopoulos, A. Baltopoulos, M. Matzakou, A. Vavouliotis, V. Kostopoulos, Electrical conductivity of polyurethane/MWCNT nanocomposite foams, Polym. Compos., 33 (2012) 1302-1312.
[34] L. Madaleno, R. Pyrz, A. Crosky, L.R. Jensen, J.C.M. Rauhe, V. Dolomanova, A.M.M.V. de Barros Timmons, J.J. Cruz Pinto, J. Norman, Processing and characterization of polyurethane nanocomposite foam reinforced with montmorillonite–carbon nanotube hybrids, Compos. Part. A: Appl. Sci. Manuf., 44 (2013) 1–7.
[35] M.C. Saha, M.E. Kabir, S. Jeelani, Enhancement in thermal and mechanical properties of polyurethane foam infused with nanoparticles, Mat. Sci. Eng., A., 479 (2008) 213-222.
[36] G. Harikrishnan, S.N. Singh, E. Kiesel, C.W. Macosko, Nanodispersions of carbon nanofiber for polyurethane foaming, Polymer, 51 (2010) 3349-3353.
[37] M.C. Saha, B. Barua, S. Mohan, Study on the Cure Kinetic Behavior of Thermosetting Polyurethane Solids and Foams: Effect of Temperature, Density, and Carbon Nanofiber, J. Eng. Mater. Technol., 133 (2011) 011015.
[38] M.E. Kabir, M.C. Saha, S. Jeelani, Effect of ultrasound sonication in carbon nanofibers/polyurethane foam composite, Mater. Sci. Eng., A., 459 (2007) 111-116.
[39] E. Thostenson, C. Li, T. Chou, Nanocomposites in context, Compos. Sci. Technol., 65 (2005) 491-516.
[40] Y.S. Kim, R. Davis, A.A. Cain, J.C. Grunlan, Development of layer-by-layer assembled carbon nanofiber-filled coatings to reduce polyurethane foam flammability, Polymer, 52 (2011) 2847-2855.
[41] IsoPMDI 92140 Technical Data Sheet. BASF Poliuretanos Iberia S.A.
[42] Elastopor H 1501/2 Technical Data Sheet. BASF Poliuretanos Iberia S.A.
[43] Pyrograf® III PR-24-XT-PS Carbon Nanofibers, in: A.S. Inc. (Ed.).
[44] ASTM D1622-08: Standard Test Method for Apparent Density of Rigid Cellular Plastics.
[45] ASTM D6226-10: Standard Test Method for Open Cell Content of Rigid Cellular Plastics.
[46] J. Pinto, E. Solorzano, M.A. Rodriguez-Perez, J.A. de Saja, Characterization of the cellular structure based on user-interactive image analysis procedures, J. Cell. Plast., 49 (2013) 555–575.
[47] UNE-EN 12667:2002. Thermal performance of building materials and products. Determination of thermal resistance by means of guarded hot plate and heat flow meter methods. Products of high and medium thermal resistance.
[48] ASTM D1621: Standard Test Method for Compressive Properties Of Rigid Cellular Plastics.
[49] R.A. Campo-Arnáiz, M.A. Rodríguez-Pérez, B. Calvo, J.A. de Saja, Extinction coefficient of polyolefin foams, J. Polym. Sci. Part B: Polym Phys, 43 (2005) 1608-1617.
[50] H.R.N. Jones, Radiation Heat Transfer, Oxford Science, Oxford, 2000.
[51] J. Shen, X. Han, L.J. Lee, Nanoscaled Reinforcement of Polystyrene Foams using Carbon Nanofibers, J. Cell. Plast., 42 (2016) 105-126.
[52] J.R. Howell, R. Siegel, M.P. Mengu, Thermal radiation heat transfer, 5th ed., CRC press2010.
[53] O. Almanza, M.A. Rodríguez-Pérez, J.A. de Saja, The Thermal Conductivity of Polyethylene Foams Manufactured by a Nitrogen Solution Process, Cell. Polym., 18 (1999) 385-401.
[54] M.A. Rodríguez-Pérez, O. Alonso, J. Souto, J.A. de Saja, Thermal Conductivity of Crosslinked Closed Cell Polyolefin Foams, Polym. Test., 16 (1997) 287-298.
[55] E. Solórzano, M.A. Rodriguez-Perez, J. Lázaro, J.A. de Saja, Influence of Solid Phase Conductivity and Cellular Structure on the Heat Transfer Mechanisms of Cellular Materials: Diverse Case Studies, Adv. Eng. Mater., 11 (2009) 818-824.
[56] L. Gibson, M. Ashby, Cellular solids: structure and properties, Pergamon Press, Oxford, 1988.
[57] T. Widya, C. Macosko, Nanoclay-Modified Rigid Polyurethane Foam, J. Macromol. Sci. Part B: Physics., 44 (2005) 897-908.

[58] M. Santiago-Calvo, V. Blasco, C. Ruiz, R. París, F. Villafañe, M.Á. Rodríguez-Pérez, Synthesis, characterization and physical properties of rigid polyurethane foams prepared with poly(propylene oxide) polyols containing graphene oxide, Eur. Polym. J., 97 (2017) 230-240.
[59] M. Santiago-Calvo, J. Tirado-Mediavilla, J.L. Ruiz-Herrero, M.Á. Rodríguez-Pérez, F. Villafañe, The effects of functional nanofillers on the reaction kinetics, microstructure, thermal and mechanical properties of water blown rigid polyurethane foams, Polymer, 150 (2018) 138-149.

Supplementary material

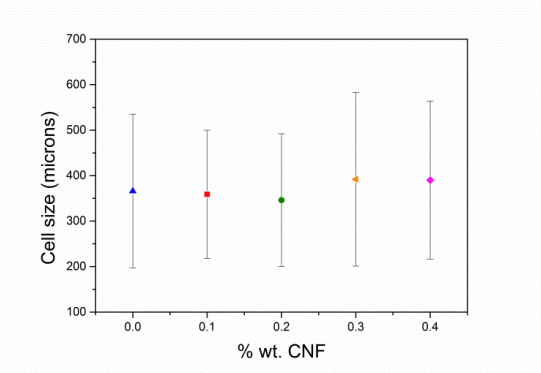

Figure S1. Average cell size vs the CNFs ratio.

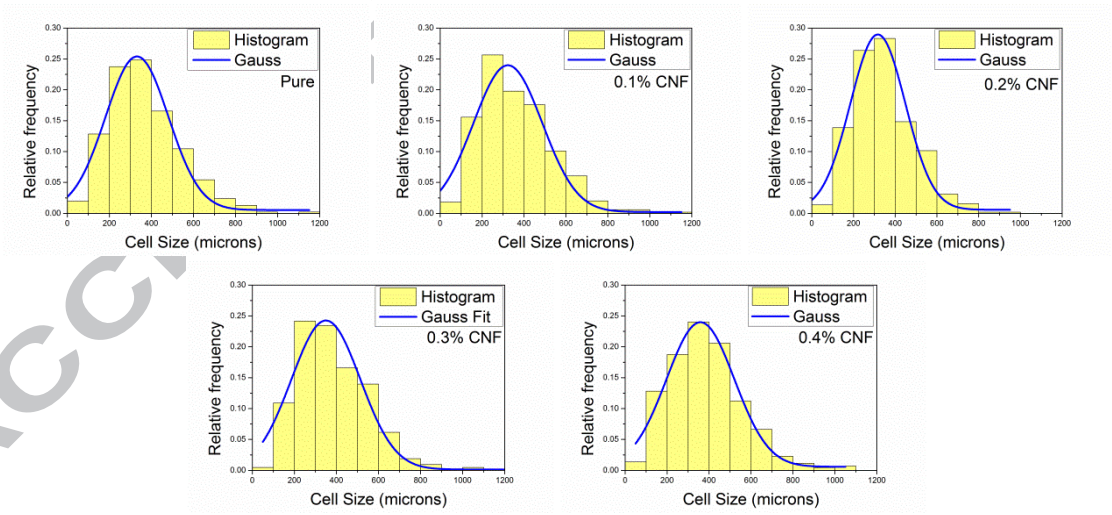

Figure S2. Cell size distribution of the foams under study.

Graphical abstract

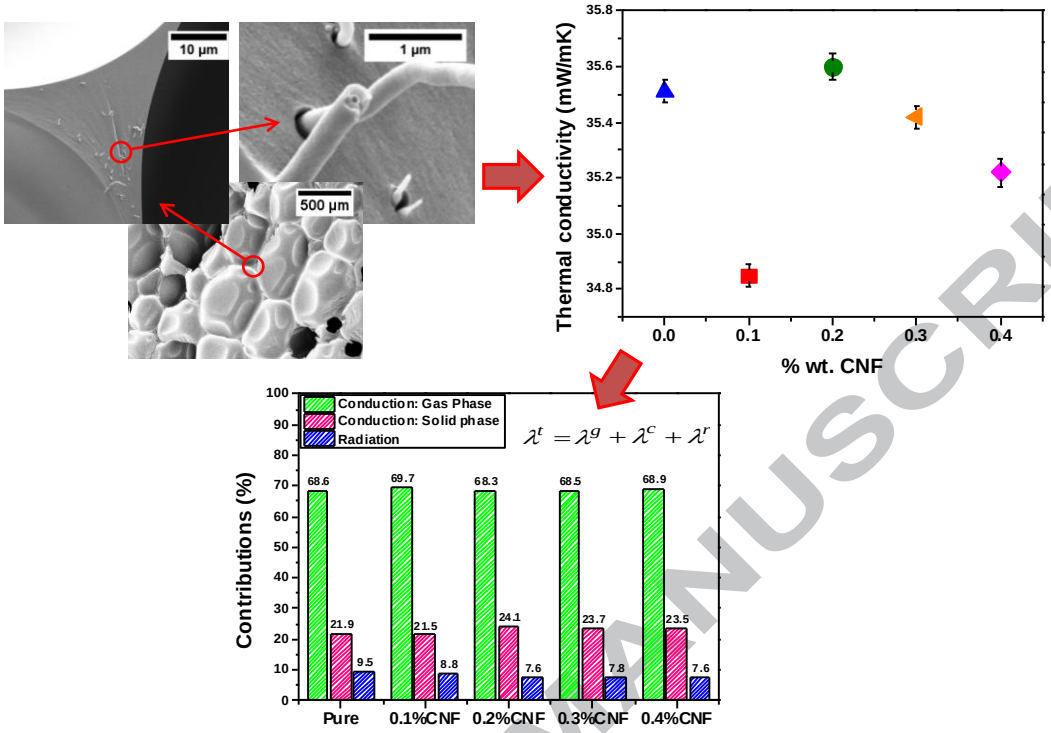

HIGHLIGHTS

- Rigid polyurethane (PUR) foams with CNFs (0.1, 0.2, 0.3 or 0.4 wt. %) are prepared and characterized.
- Thermal conductivity is improved with only 0.1 wt. % of CNFs.
- Thermal conductivity changes are explained by measuring the extinction coefficient and by using a theoretical model.
- Mechanical properties are maintained or improved in the PUR foam with 0.1 wt. % of CNFs.